DEEP LEARNING AND WBG DEVICES COMBINING TO IMPROVE PV SYSTEM EFFICIENCY: ANFIS-BASED MPPT CONTROLLER

ELAID BOUCHETOB, BOUCHRA NADJI

Keywords: Adaptive neuro-fuzzy inference system (ANFIS); Photovoltaic (PV) system; Silicon carbide (SiC) devices; Efficiency; Ansys.

With the escalating demand for renewable energy sources, photovoltaic (PV) systems have emerged as a pivotal solution for sustainable power generation. The efficacy of these systems is paramount for their widespread implementation. This research article delves into the efficiency assessment of silicon carbide (SiC) components within a boost converter integrated into a PV system. Notably, the boost converter switch is under the intelligent control of an adaptive neuro-fuzzy inference system (ANFIS) based maximum power point tracking (MPPT) controller. This innovative approach leverages AI to optimize energy extraction from PV panels, thereby enhancing overall system efficiency. The cooperation of SiC components and AI-driven control presents a novel perspective on robust and efficient PV systems. To substantiate the research, data collected from the Sidi Bel-Abès PV central is utilized to train the ANFIS. The utilization of real-world data enhances the accuracy of the predictive model, thereby increasing its applicability to practical scenarios. Integrating AI technologies with PV systems marks a significant advancement toward intelligent and adaptive energy systems.

1. INTRODUCTION

In recent years, the global transition to sustainable energy has driven nations to adopt innovative solutions that align environmental goals with technological progress. Algeria, leveraging its abundant solar potential, has adopted this shift through strategic projects, such as the Sidi Bel-Abbès photovoltaic (PV) central, which exemplifies the country's commitment to renewable energy deployment and clean electricity generation. Beyond national initiatives, the success of such PV systems depends on continual improvements in power conversion efficiency and intelligent control strategies.

Among the most promising technological advancements, the integration of Silicon Carbide (SiC) devices belonging to the wide bandgap (WBG) semiconductor family into DC-DC boost converters has shown great potential in enhancing photovoltaic system performance. Prior studies [1] have demonstrated that SiC devices significantly reduce switching losses, improve thermal management[2], and increase efficiency compared to traditional silicon-based converters. A comparative study further highlighted the superiority of SiC devices in PV boost converter applications [3].

Concurrently, Artificial Intelligence (AI) has revolutionized PV system optimization, particularly in areas such as Maximum Power Point Tracking (MPPT), fault detection, and adaptive control[3]. Among the advanced AI methods, Adaptive Neuro-Fuzzy Inference System (ANFIS) stands out as a powerful hybrid approach that combines the learning capabilities of neural networks with the reasoning structure of fuzzy logic. This synergy allows ANFIS to model highly nonlinear and time-varying systems, making it particularly effective in dynamic and uncertain environments such as solar energy systems.

ANFIS offers several advantages over conventional controllers, including rapid adaptation to changing environmental conditions (irradiance and temperature), superior approximation capabilities, and improved convergence in MPPT tasks. Its ability to learn from historical data while handling ambiguity and imprecision

makes it well-suited for real-time control and optimization of PV systems[4]. Recent implementations in the power electronics domain have shown that ANFIS can significantly improve the performance of power factor correction circuits in single-phase boost converters, achieving better efficiency and quicker adaptation to varying operational conditions[5]. Despite its proven effectiveness, few studies have explored its integration with high-performance power converters based on Wide Bandgap (WBG) materials, especially in PV systems [1].

This study addresses that critical gap by proposing a hybrid model that combines a SiC-based DC-DC boost converter with an ANFIS controller. Through comprehensive simulation and performance evaluation, the proposed system demonstrates enhanced conversion efficiency, faster dynamic response, and greater stability under variable operating conditions, thus contributing to the development of intelligent, high-performance PV systems.

By bridging the domains of power electronics and AI-driven control, this research contributes to the next generation of intelligent and efficient PV systems, particularly in high-potential regions like Algeria.

2. MATERIAL AND METHODS

2.1 SIDI BELABESS PV CENTRAL

The Sidi Bel Abbès solar energy facility serves as a notable example of renewable energy innovation, utilizing HSL60P6/250WC-DC panels, which are known for their efficiency and reliability. The facility is equipped with 12 inverters connected to 3984 modules, generating a total output of 12 MW. The configuration includes two strings of 24 modules in series, with 83 modules in parallel per string, optimizing energy extraction and ensuring operational stability. This facility reflects a strong commitment to harnessing solar power to address current energy needs and long-term sustainability goals.

In the current study, focus is placed on four PV panels, each producing 1000W. These panels drive the energy generation process, with their characteristics influencing the study's results (Table 1). The generated power is fed into a SiC-based DC-DC boost converter, designed to step

E-mail: e.bouchetob@univ-boumerdes.dz, b.nadjiouchetob@univ-boumerdes.dz

¹ Faculté des hydrocarbures et de la chimie, Laboratoire d'électrification des entreprises industrielles (LREEI), Université de M'hamed Bougara, Boumerdès, Algérie.

up the voltage to 400V, with its parameters detailed in Table 2.

Table 1
PV panel parameters

| 1 v paner parameters | | | | | |
|----------------------------------|--------|-------|--|--|--|
| Parameter | Symbol | Value | | | |
| Maximum power (W) | Pmpp | 250 | | | |
| Voltage @ Pmpp (V) | Vmpp | 30.4 | | | |
| Current @ Pmpp (A) | Impp | 8.23 | | | |
| Short circuit current (A) | Isc | 8.79 | | | |
| Open voltage current (V) | Voc | 37.7 | | | |
| Temperature coefficient of open | В | -0.31 | | | |
| circuit voltage (%/°C) | | | | | |
| Temperature coefficient of short | A | +0.05 | | | |
| circuit current (%/°C) | | | | | |
| Surface (m ²) | S | 1.62 | | | |
| Number of series cells | Ns | 60 | | | |
| | | | | | |

Table 2
DC-DC boost converter parameters

| Parameter | Device specification |
|-----------------------------|----------------------|
| Inductor (mH) | 1.7 |
| Capacitor (μF) | 21.8 |
| Resistor (Ω) | 160 |
| Input voltage(V) | 121 |
| Output voltage(V) | 400 |
| Estimate ripple current (A) | 1.65 |
| Switch frequency(kHz) | 20 |
| Duty cycle | 0.697 |
| Estimate ripple voltage(V) | 8 |

2.2 SIC SEMICONDUCTOR DEVICES

SiC (silicon carbide) power devices are advanced semiconductor components used in power electronics for applications like electric vehicles, renewable energy systems, and industrial motor drives. Made from silicon carbide, these devices offer several advantages over traditional silicon-based devices, including a higher breakdown voltage, better thermal conductivity, and a wider operating temperature range, making them suitable for harsh environments[6].

One of their key benefits is lower switching losses, allowing them to switch faster and more efficiently, which reduces energy loss and the size and weight of power electronics systems. While SiC devices are still more expensive than silicon-based alternatives, their superior efficiency and performance make them increasingly popular across various industries.

Table 3
Power devices parameters

| Manufacture | ST | APT | Microsemi | Infineon Tech |
|-----------------------------------|----------------|-------------------|-------------------|------------------|
| Part number | SCT30 N120 | APT1206 0B2VRF | APT2X21 DC120J | IDP18E120 |
| Breakdown voltage (v) rated | 1200 | 1200 | 1200 | 1200 |
| Rated current (i) | 34 @ 100 °C | 20@25°C | 20@100°C | 31@25°C |
| Maximum junction temperature (°C) | 200 | 150 | 175 | 150 |
| Gate-source voltage | - 10/+20 | -30/+30 | / | / |

2.3 AI (ANFIS) BASED MPPT CONTROLLER

ANFIS-based MPPT controllers are increasingly popular for optimizing power output in solar PV systems. By combining fuzzy logic and neural networks, they continuously monitor solar panel output and adjust voltage.

They also enable the current to be maintained at the maximum power point, based on past performance data. This results in improved accuracy, efficiency, and adaptability, especially under conditions like shading or partial sunlight. Although they are more complex and may require additional components, their benefits in energy efficiency and lower operating costs make them a valuable investment for solar installations. ANFIS-based controllers are a promising area of research in optimizing PV systems.

The equations used in the ANFIS-based MPPT algorithm can be broken down into the following steps:

Step 1: Fuzzification of Inputs:

Input variables are transformed into fuzzy values using Gaussian membership functions, which determine how strongly an input belongs to a linguistic term (*e.g.*, "low," "medium," "high").

For each input variable x_i (where i = 1,2,3,....,n), fuzzify the input using Gaussian membership functions:

$$\mu_{Ai}(x_i) = \exp\left(-\frac{(x_i - ci_i)}{2\sigma_i^2}\right),\tag{1}$$

where c_i is the center of the ith Gaussian membership function, and σ_i is the standard deviation of the ith Gaussian membership function.

Step 2: Rule Activation:

The activation weight of each rule is computed by multiplying the membership values of the associated input variables, indicating the "firing strength" of each rule.

Combine the fuzzified inputs to compute the activation weight of each rule Rj:

$$\omega_j = \prod_{i=1}^n \mu_{Ai}(x_i). \tag{2}$$

Step 3: Normalization:

The activation weights are normalized so that their sum equals 1, converting them into fuzzy probabilities.

Normalize the activation weights of the rules:

$$\omega_{j}^{'} = \frac{\omega_{j}}{\sum_{j=1}^{m} \omega_{j}},\tag{3}$$

where m is the total number of rules.

Step 4: Inference:

The consequent parameters of each rule are computed, representing the output of the rule based on the input variables.

For each rule Rj, compute the consequent parameter y_j using a linear or nonlinear function:

$$y_j = p_{0j} + p_{1j}x_1 + \dots + p_{nj}x_n. \tag{4}$$

Step 5: Defuzzification:

The outputs of all rules are combined using the weighted average, with normalized firing strengths as weights, to generate a single crisp output.

Combine the consequent outputs of all the rules to produce the final output:

$$\hat{y} = \frac{\sum_{j=1}^{m} (\omega_{j}' y_{j})}{\sum_{j}^{m} \omega_{j}'}.$$
 (5)

Step 6: Parameter Adaptation:

The parameters of the membership functions and consequent parameters are adjusted using a learning algorithm (like gradient descent) to minimize the error between the actual and desired output.

$$\Delta c_i = -\eta \frac{\partial E}{\partial c_{ij}} \tag{6}$$

$$\Delta \sigma_i = -\eta \frac{\partial E}{\partial \sigma_{ij}} \tag{7}$$

where η is the learning rate and E is the error.

Step 7: Output Adjustment:

The consequent parameters are fine-tuned using gradient descent to minimize the error and optimize the output.

$$\Delta p_i = -\eta \frac{\partial E}{\partial p_{ij}} \tag{8}$$

where E is the error.

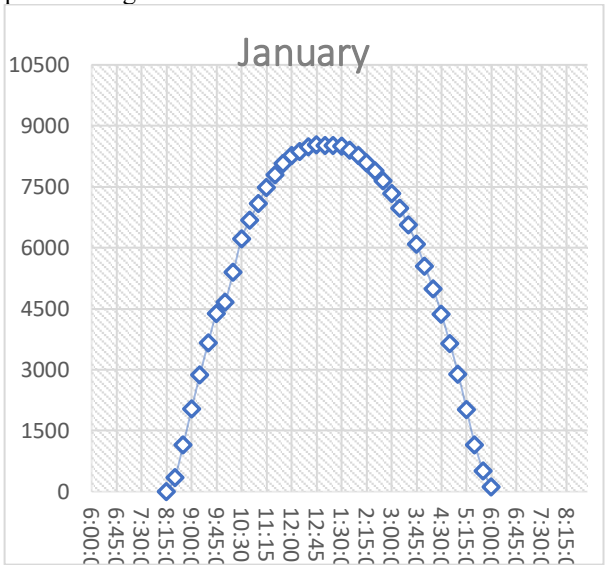
Step 8: Training:

The ANFIS model learns iteratively from the training dataset, refining its parameters over multiple epochs to improve prediction accuracy.

Step 9: Evaluation:

After training, the model makes predictions on unseen data, going through fuzzification, rule activation, inference, and defuzzification to produce the final output.

Data used for training the ANFIS controller was collected from the central for one year (2021). We have used Irradiance and temperature as inputs, and the output is the panel voltage.



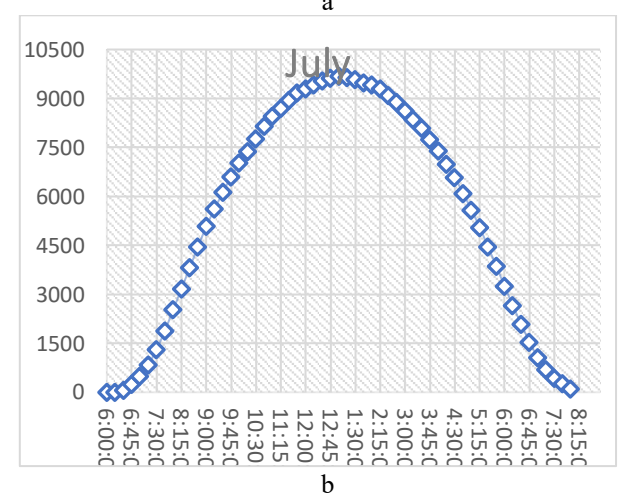


Fig. 1 – ANFIS controller architecture.

The power production data from Sidi Bel Abbès Central reveals that in January, power output gradually increases

starting around 8:00 AM, peaking at approximately 8,700 watts at midday. This slower rise is attributed to the lower sun angle and shorter daylight hours. In contrast, July experiences a quicker rise beginning at 6:30 AM, with a higher peak of 10,200 watts earlier in the day, driven by stronger solar radiation and longer sunlight hours. While both months show similar patterns, the July curve demonstrates a more rapid and intense increase in power production, resulting in a higher peak compared to January's more gradual rise and lower peak. This data was used to generate the ANFIS controller, optimizing the power production of the PV system.



Fig. 2 – ANFIS controller architecture.

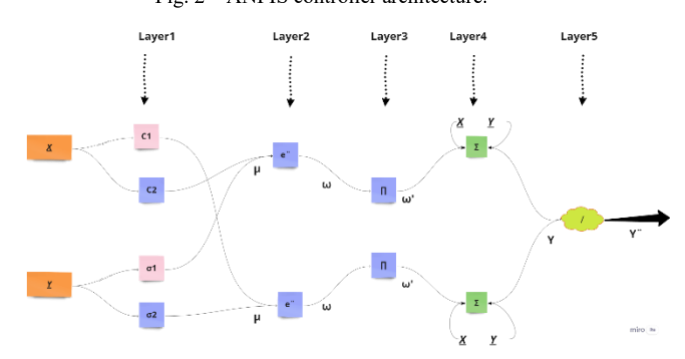


Fig. 3 - Output results for ANFIS.

We used one year of data collected from the central system to train the adaptive neuro-fuzzy inference system (ANFIS) controller. After training the model, the results are illustrated in Fig. 3.

In this figure, the blue line represents the expected output (target data), while the red line indicates the ANFIS predicted output during training. It is evident that the predicted output closely follows the expected values, with minimal deviation. This indicates a high level of accuracy in the learning process and confirms that the ANFIS controller has successfully captured the underlying data patterns.

The smooth alignment between predicted and actual values demonstrates the model's ability to generalize, making it suitable for reliable performance in further testing and real-world implementation. Overall, this figure validates the effectiveness of the training phase for our ANFIS-based control system.

2.4 SIMULATED MODEL

The co-simulation framework integrates the strengths of MATLAB Simulink and ANSYS Simplorer, modeling a complex PV system with a SiC-based boost converter and AI-driven MPPT control. Using Sim2Sim and AnsoftSFunction interfaces, data flows seamlessly between the tools. Simulink models the PV panels and ANFIS-based MPPT algorithm, while Simplorer simulates the boost converter. During co-simulation, data is exchanged bidirectionally, enabling dynamic interaction and in-depth

analysis of the system's behavior. This method provides valuable insights into the converter's operation, the Alcontrolled MPPT, and the panel's responses. While the approach provides a comprehensive view, it requires careful configuration and may face challenges in communication synchronization and debugging. Overall, this framework combines specialized capabilities for accurate modeling and realistic exploration of the PV system's efficiency and reliability.

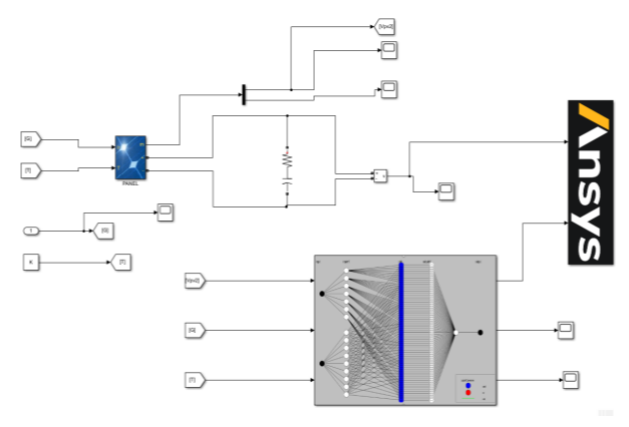


Fig. 4 – MATLAB simulated model.

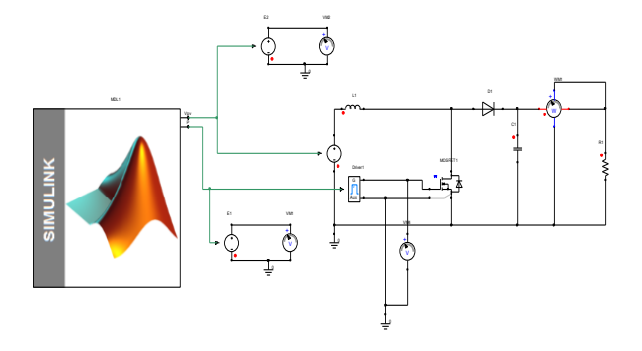
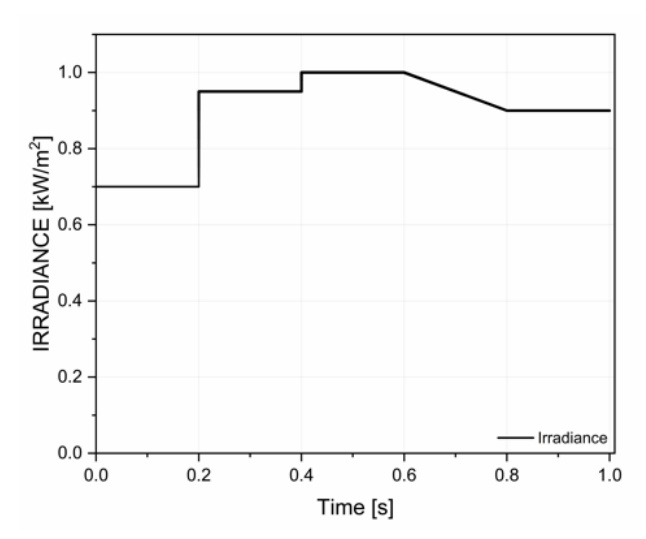


Fig. 5 – Ansys simulated model.



 $Fig.\ 6-Dynamic\ changes\ in\ irradiance.$

We have incorporated tests to evaluate the reliability of the ANFIS MPPT controller under partial shading conditions. Figure 6 presents the dynamic changes in irradiance applied to the system, simulating various scenarios to evaluate the performance of the MPPT algorithm. These scenarios encompass both gradual and rapid changes in irradiance, simulating the effects of partial shading on the PV system.

- Between 0 seconds < t < 0.2 seconds, a smooth and significant change in irradiance is applied, evaluating the algorithm's adaptability to partial shading.
- At t = 0.2 seconds, a fast and significant change in irradiance is simulated, which challenges the responsiveness of the MPPT controller under partial shading conditions.
- At t = 0.4 seconds, a fast but smaller change in irradiance is tested, assessing the algorithm's agility in tracking the maximum power point under partial shading.
- Between 0.6 seconds < t < 0.8 seconds, another smooth and significant change in irradiance unfolds, further testing the algorithm's adaptability under varying irradiance caused by partial shading.
- During fixed input with low irradiance between 0 < t
 < 0.2 seconds and 0.8 < t < 1 seconds, the algorithm demonstrates its stability under consistent shading conditions.
- Fixed changes with high irradiance between 0.2 < t < 0.4 seconds and 0.4 < t < 0.6 seconds assess the tracking efficiency of the algorithm under partial shading.

Through these simulations, we have ensured a comprehensive evaluation of the ANFIS controller's ability to handle partial shading, providing insights into its reliability and adaptability under real-world conditions. These tests demonstrate that the ANFIS controller remains effective in tracking the maximum power point even when subjected to partial shading, further validating its robustness in dynamic environments.

3. RESULTS AND DISCUSSION

Efficiency is a critical metric in power electronics systems, directly impacting energy conversion and system performance. The comparison of power efficiency between the SiC-based and Si-based boost converters reveals a significant advantage for the SiC system. The SiC-based boost converter consistently maintains higher efficiency levels across a wide range of load conditions. This efficiency gain is attributed to the inherent properties of SiC devices, including their lower conduction losses and reduced switching losses.

In the realm of power electronics systems, efficiency is a paramount metric, serving as a barometer of energy conversion efficacy and overall system performance. In the context of our investigation, we focus on the power output efficiency of SiC-based and Si-based boost converters.

The power output profiles in Fig. 7 illustrate a clear efficiency advantage for the SiC-based boost converter compared to its Si-based counterpart under varying load conditions—this efficiency enhancement results from SiC's superior material properties, which reduce both conduction and switching losses. SiC devices can handle higher current densities with lower resistive losses, and their faster switching capabilities minimize energy dissipation, resulting in improved overall efficiency.

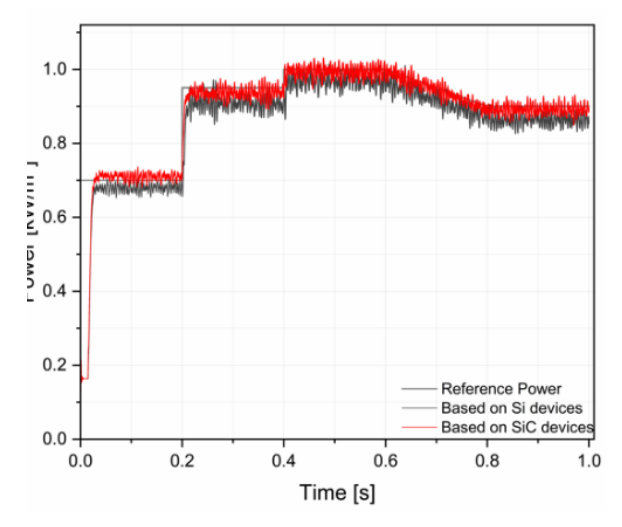
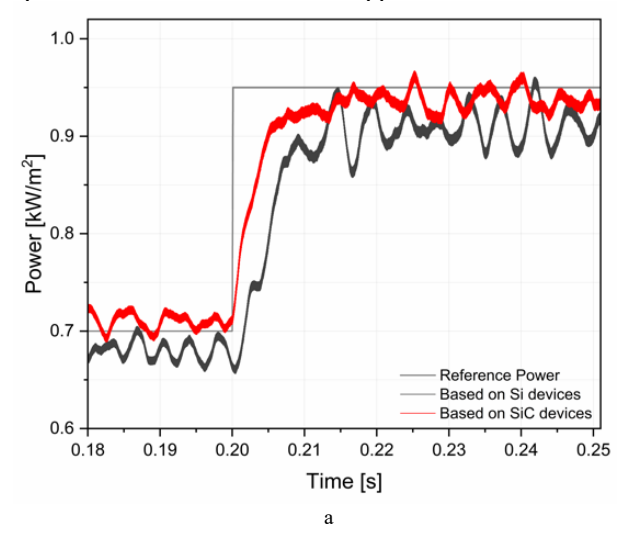


Fig. 7 – Comprehensive power output comparison.

The SiC-based converter maintains a higher power output efficiency across its operational range, highlighting the significant impact of SiC technology on power electronics. This improvement in efficiency positions the SiC-based converter as a key player in achieving more sustainable power conversion systems with energy savings and enhanced performance.

Voltage and current waveforms, crucial indicators of system performance, further emphasize the SiC converter's advantages. The SiC system exhibits superior current response, featuring faster rise and fall times, as well as reduced ripple, which leads to enhanced power conversion efficiency. These benefits stem from the high-frequency switching capability of SiC devices, resulting in less wasted energy and a more stable system.

Moving forward, we explore the intricate relationship between the adaptive neuro-fuzzy inference system (ANFIS) algorithm's rapid response and the efficiency dynamics of the SiC-based boost converter. As shown in Figures 8(a), 8(b), and 8(c), the ANFIS algorithm effectively adapts to varying irradiance conditions, quickly adjusting to changes in power demand while efficiently tracking the maximum power point. This agility leads to optimized energy extraction, positioning the ANFIS-controlled SiC-based boost converter as a responsive solution for real-world applications.



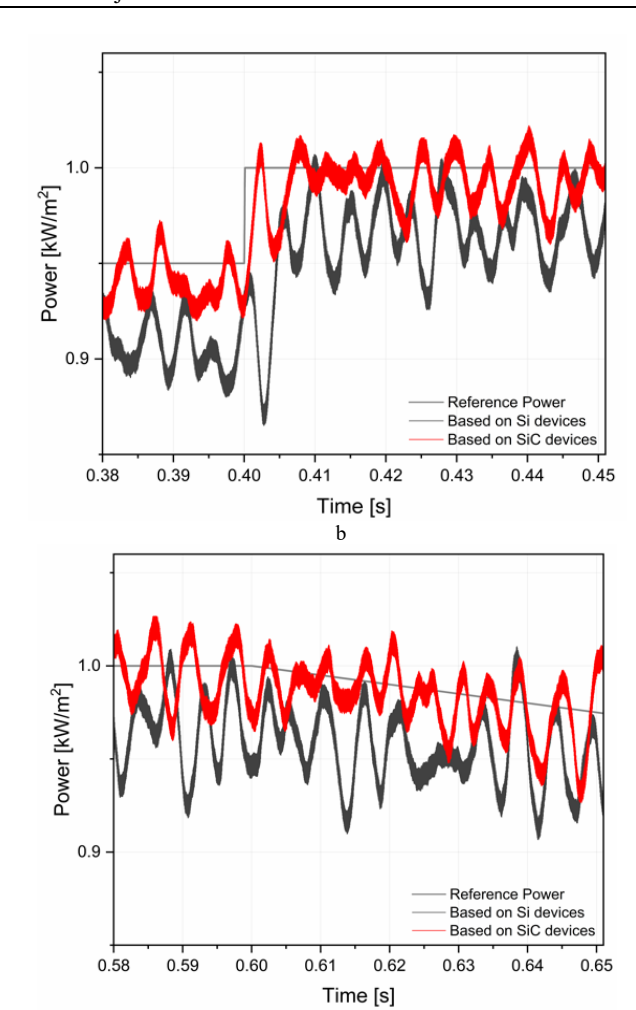
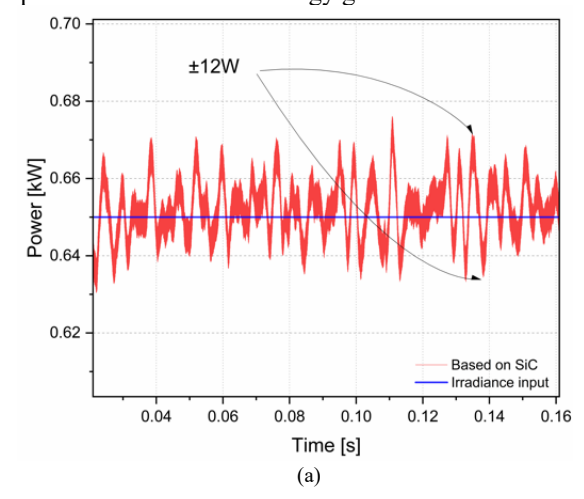


Fig. 8 – (a, b, c) Comprehensive power output waveform comparison for different times.

Figures 8(a), 8(b), and 8(c) further illustrate the converter's efficiency under dynamic conditions, highlighting its ability to maintain high power efficiency. The collaboration between SiC devices and ANFIS control enhances system performance by minimizing losses and optimizing power conversion. Together, the ANFIS algorithm and SiC technology form a dynamic, efficient power electronics system capable of adapting to the complexities of renewable energy generation.



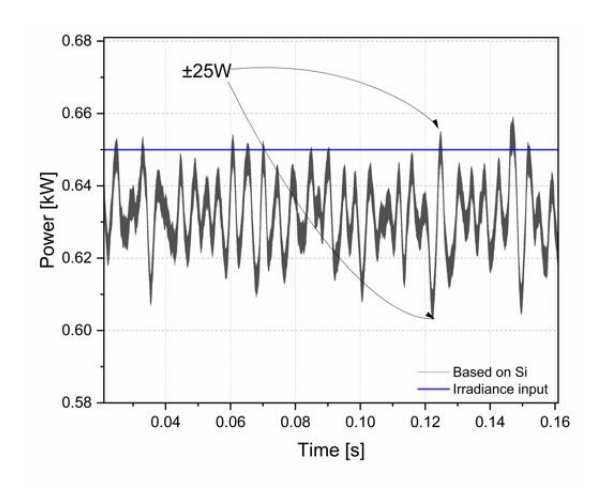


Fig. 10 – (a, b) Comprehensive power output waveform comparison for different times.

The effectiveness of the maximum power point tracking (MPPT) technique is crucial in various PV applications, including satellite power supplies, spacecraft, and large-scale PV plants. The MPPT performance was quantitatively evaluated through simulations, showing the system's stable response. Efficiency can also be calculated using the following formula.

Waveform oscillations in a boost converter, caused by factors such as load fluctuations, switching transitions, or component variations, can negatively affect its reliability. These oscillations increase stress on the components, accelerating wear and reducing their lifespan. The issue is exacerbated by thermal stress, resulting in higher energy losses and increased operating temperatures. Voltage and current spikes from these oscillations may also exceed component limits, potentially causing insulation breakdown and compromising overall reliability.

$$\eta_{\text{tech}} = \frac{1}{m} \sum_{i=0}^{m} \frac{P_j}{P_{\text{max},j}} \tag{9}$$

The equation becomes:

$$\eta_{tech} = \frac{1}{m} \sum_{i=0}^{m} 1 - \frac{P_{s}}{P_{\max,j}}$$
 (10)

while

$$P_{\rm s} = P_{\rm max.i} - P_{\rm i} \tag{11}$$

where, η_{tech} is the technique efficiency, m is the number of samples, Ps is the squandered, and Pi is the panel power.

Figure 11 shows the converter efficiency of SiC-based and Si-based devices across various switching frequencies.

The SiC-based converter maintains high efficiency above 96%, even at 100 kHz, while the Si-based converter shows a noticeable drop, falling below 89%. This demonstrates the better high-frequency performance of SiC devices, making them more suitable for efficient, high-speed power conversion.

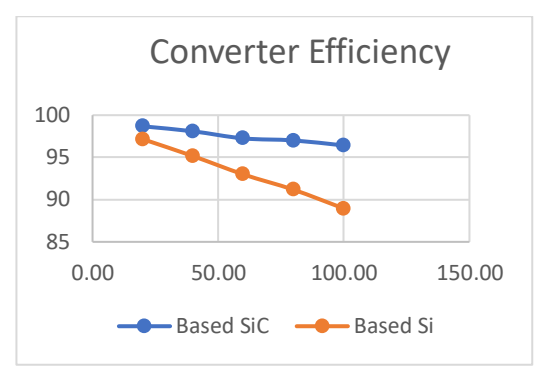


Fig. 11 – (a, b) Comparative converter efficiency.

4. CONCLUSION

This study presents a comprehensive efficiency assessment of a PV system integrating a SiC-based DC-DC boost converter controlled via an ANFIS-based MPPT algorithm. Compared to conventional silicon-based systems, the SiC configuration demonstrated a notable increase in tracking efficiency (up to 98.6%) and a reduction in ripple and response time. The ANFIS controller also demonstrated strong adaptability under partial shading, maintaining an efficiency of over 97%.

These results confirm the synergistic advantage of combining WBG materials with intelligent control algorithms. By bridging the gap between AI-driven MPPT and advanced power electronics, this research contributes a scalable and efficient solution for next-generation PV systems. Future work may extend to real-time hardware-in-the-loop (HIL) implementations to validate field applicability.

CREDIT AUTHORSHIP CONTRIBUTION

Elaid Bouchetob: simulation, writing,

Bouchra Nadji: references, language correction.

REFERENCES

- E. Bouchetob, B. Nadji, I. Mahdi, Efficiency comparison of silicon and silicon carbide MOSFETs in a PV system application, International Conference on Advances in Electronics, Control and Communication Systems (ICAECCS), BLIDA, pp. 1-6 (2023).
- E. Bouchetob, B. Nadji, Boosting reliability: a comparative study of silicon carbide (Sic) and Silicon (Si) in boost converter design using MIL-HDBK-217 Standards, Int. J. of Electrical and Computer Eng. Systems, 15, 4, pp. 313–320 (2024).
- S. Latreche, A. Bouafassa, B. Babes, O. Aissa, Efficient DSP-based real-time implementation of anfis regulator for single-phase power factor corrector, Rev. Roum. des Sci. Tech. Ser. Electrotech. Energ., 69, 2, pp. 141–146 (2024).
- N. Kalaiarasi, S.S. Dash, S. Paramasivam, C. Bharatiraja, Investigation on ANFIS aided MPPT technique for PV fed ZSI topologies in standalone applications, J. Appl. Sci. Eng., 24, 2, pp. 261–269 (2021).
- B. Babes et al., A dSPACE-based implementation of ANFIS and predictive current control for a single-phase boost power factor corrector, Sci. Rep., 14, I, pp. 1–21 (2024).
- A. Awasthi et al., Review on sun tracking technology in solar PV system, Energy Reports, 6, pp. 392–405 (2020).